Journal of Thermal Analysis, Vol. 46 (1996) 1301-1311

THERMAL BEHAVIOR OF ALKALI METAL AZIDES IN NaY–FAU ZEOLITE

A. Béres, I. Hannus and I. Kiricsi

Applied Chemistry Department, József Attila University, H-6720 Szeged, Hungary

(Received January 7, 1995; in revised form April 5, 1995)

Abstract

The thermal behavior of pure alkali metal azides and their mechanical mixtures with NaY–FAU zeolite was investigated by means of thermogravimetry and IR spectroscopy. LiN_3, KN_3, RbN_3 and CsN_3 were prepared from NaN_3 by ion-exchange. The pure azides exhibited low thermal stability, hindering the precise spectroscopic characterization in some cases. The decomposition of each azide in the zeolite took place above the temperature characteristic for the pure azide, demonstrating the stabilization of the azide in the zeolite cavities. This feature was the only common characteristic established for the azide/zeolite systems.

Keywords: alkali metal azides, zeolite

Introduction

For several years we have investigated the thermal behavior of NaN_3 in zeolites by applying various experimental techniques. The decomposition of NaN_3 in zeolites occurred at higher temperature than that for pure NaN_3 [1]. When the NaN_3 was loaded from solution by impregnation of the zeolite, some of the NaN_3 introduced into the zeolite (2 mol NaN_3 per unit cell) did not decompose, but remained occluded in the cavities [2]. The IR spectra taken in the course of this salt occlusion process exhibited several absorptions, the positions of which depended strongly on the conditions of sample preparation [3]. These findings were recently confirmed by the group of Förster [4]. They proved that the decomposition temperature of NaN_3 depended on (i) the concentration of NaN_3 in the zeolite and (ii) the Si/Al ratio of the zeolite matrix. ^{23}Na NMR spectra taken after decomposition of the NaN_3 revealed the formation of neutral sodium clusters, while the ESR spectra registered after identical pretreatment permitted the assumption of the generation of both neutral and charged sodium clusters [5]. In general, our conclusions were in agreement with those obtained by the group of Martens [6, 7].

0368–4466/96/ $ 5.00

John Wiley & Sons, Limited
Chichester

Kevan and co-worker have reported on the ESR characterization of metal complexes generated by the interaction of alkali metal (designated as M) vapor and MX-FAU zeolites exchanged for alkali or alkaline-earth metal ions [8]. In their study, alkali metal vapor was produced by thermal decomposition of the respective azide salt, which was either applied to the zeolite from methanol solution or placed on a separate holder under the zeolite layer. They concluded that the entering metal generated the clusters when it was smaller than K, but Rb and Cs clusters were formed when these elements were present, irrespective of whether they were entering atoms or cations in the treated zeolite.

To widen the area studied, we have now investigated the thermal behavior of alkali metal azides in NaY–FAU zeolite. The results obtained are reported in this paper.

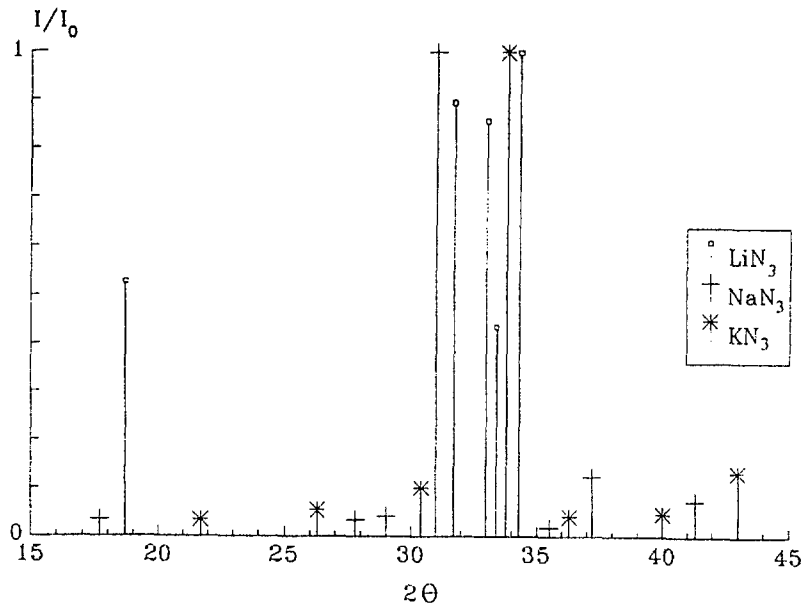

Fig. 1/A X-ray diffractograms of LiN_3, NaN_3 and KN_3

Experimental

LiN_3, KN_3, RbN_3 and CsN_3 were prepared from commercial NaN_3 via an ion-exchange procedure starting from the chlorides. Ion-exchange was performed on a column (length: 540 mm, inner diameter: 20 mm, resin volume: 170 cm^3) filled with VARION ADAM anion-exchange resin from NIKE (Hungary). A 10 cm^3/min flow rate was applied for both the ion-exchange and the regeneration, which was performed with NaN_3 solution. The first fraction of the eluent was collected and analyzed. Its water content was reduced by evapo-

ration at 353 K, followed by precipitation of the crystals with ethanol. The exception was LiN_3, where only evaporation was applied.

NaY–FAU zeolite (from UC, Linde Div.) was used without any purification. Its composition was determined by elemental analysis.

Azide-loaded zeolites were prepared by mechanical mixing of appropriate amounts of the azides with zeolite. The mixtures were intimately homogenized in an agate mortar for 1 h.

X-ray diffraction, IR spectroscopy, elemental analysis and derivatography were used to investigate the physical behavior of both the pure azides and the azide-treated zeolite mixtures.

For X-ray diffraction, well-powdered materials were prepared from the azides and the azide–zeolite mixtures. X-ray diffractograms were taken in the interval $4°<2\theta<40°$, using a DRON 3 diffractometer.

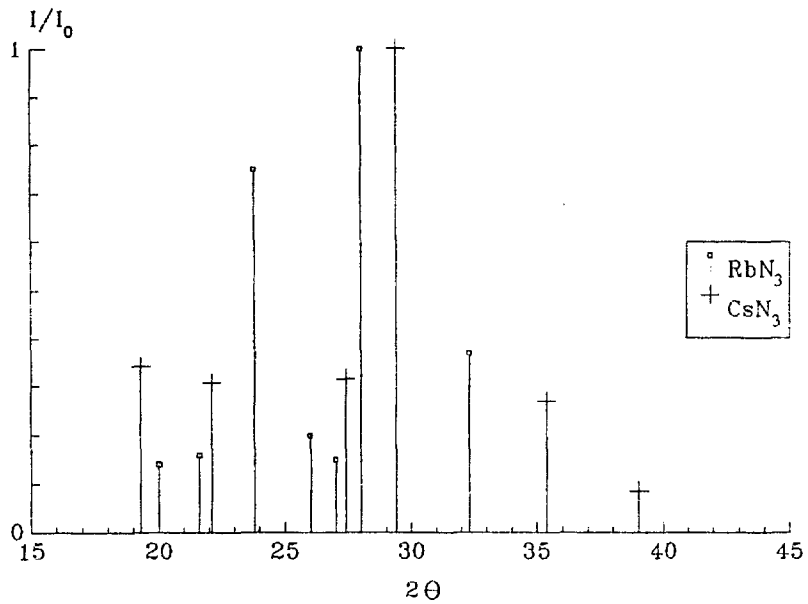

Fig. 1/B X-ray diffractograms of RbN_3 and CsN_3

IR spectroscopic measurements were run on a Genesis FTIR spectrometer (Mattson), using the KBr matrix technique. Generally, 1 mg of sample was mixed mechanically with 200 mg of KBr and pressed into a disc form. Other matrix materials, such as NaCl, RbCl and CsCl, were also applied.

For chemical analysis, atomic absorption spectroscopy and classical analytical methods were utilized.

Derivatographic measurements were performed with Hungarian-made Derivatograph Q equipment. Various heating rates were chosen in the range

298–1273 K for the different samples. Powdered materials were placed in thin layers on a plate-series holder in order to avoid sample blowing during the decomposition of azide.

Table 1 Physical characteristic of alkali metal azides

Azide	Melting points/ K	T_{decomp}/ K	
LiN_3	decomp.	508*	
NaN_3	decomp.[11]	623*	623[4], 650-680[8], 548[11]
KN_3	616[11]	683*	650-680[8], 628[11]
RbN_3	594[11], 594-613[12]	713*	668-6808, 668[11]
CsN_3	599[11], 583-599[12]	687*	663-680[8], 663[11]

[4,8,11,12]Data from references

*this work

Results and discussion

Schematic X-ray patterns of alkali metal azides are to be seen in Fig. 1. Comparisons of these data with the respective ASTM data (except for CsN_3, where no ASTM data were available) resulted in good agreement.

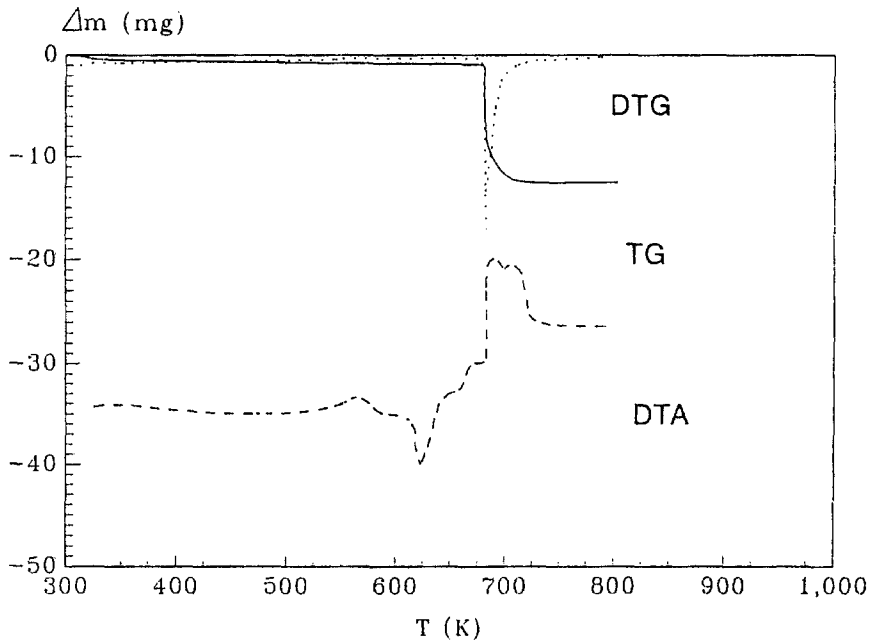

Fig. 2 Derivatographic pattern of KN_3 registered at 1.25 K min^{-1} heating rate in flow N_2

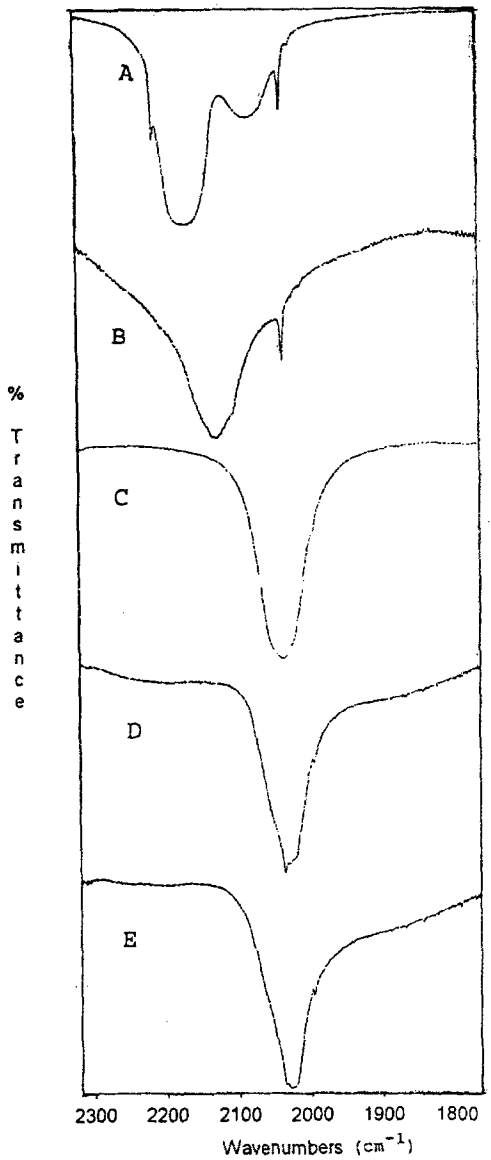

Fig. 3 IR spectra of LiN_3 (A), NaN_3 (B), KN_3 (C), RbN_3 (D) and CsN_3 (E) in KBr matrix

Table 1 lists the decomposition temperatures measured by derivatography in N_2 and also the literature data. The melting points of the alkali metal azides are included, too. It can be seen that LiN_3 and NaN_3 decomposed before melting, while definite melting points were found for the other azides. The thermogravimetric pattern of KN_3, as an example, is depicted in Fig. 2. Characteristic features of this pattern are the endothermic transformations of KN_3 due to melt-

ing at 616 K and decomposition at 683 K. LiN_3 was observed to be strongly hygroscopic and decomposed slowly even at room temperature. Great care should therefore be taken if it is stored. However, it is better to prepare a fresh sample for each experiment.

IR spectra of alkali metal azides in KBr are depicted in Fig. 3. The spectra of LiN_3 and NaN_3 display four (at 2211, 2170, 2080 and 2036 cm^{-1}) and two (at

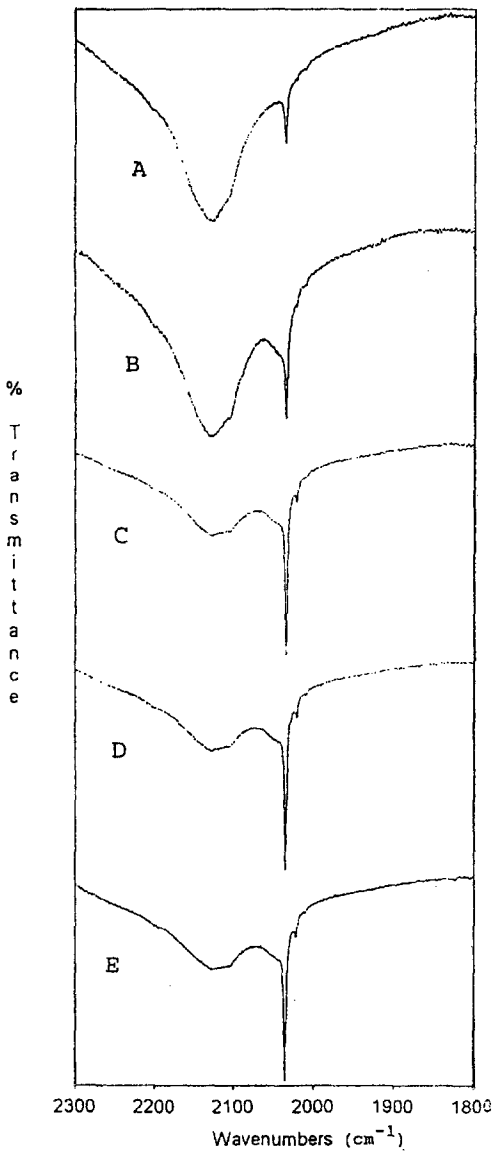

Fig. 4 IR spectra of NaN_3 in KBr matrix with increasing time of storage: fresh sample (A), after 1 day (B), 2 days (C), 3 days (D) and 4 days (E)

2130 and 2036 cm^{-1}) absorptions, respectively. These are in the region of the asymmetric stretching vibration of the azide ion [9], which varies greatly with time. This feature suggests that ion-exchange may take place between the azide and the bromide or the Li^+ and Na^+ and K^+ ions. The probability of this ion-exchange is higher for Li^+ and Na^+ than for the other alkali metal ions, due to the instability of their azides and to the fact that these materials have different crystal structures from those of the heavier azides [11]. It is also noteworthy that the absorptions in the $\nu_3+R(E_g)$ combination vibration region (2170–2130 cm^{-1}) [9] are strong if Li^+ or Na^+ is present in the system. Figure 4 depicts spectra of NaN_3 in a KBr matrix, taken after increasing waiting times. It is seen that the intensities of the bands at ~2130 and ~2036 cm^{-1} change drastically with time. This observation is regarded as convincing evidence of reactions taking place in the IR wafer itself. It follows that the spectroscopic analysis of alkali metal azides in this way is rather complicated.

Table 2 Alkali azide IR-bands in the asymmetric stretching vibration region (cm^{-1})

	Matrix			
	NaCl	KBr	RbCl	CsCl
LiN_3	2211,2170	2211,2170	2211,2166	2211,2166
	2084,2070	2080,2036	2075,2033	2070
NaN_3	2117,2105	2130,2036	2140,2105	2150,2009
	2084,2056		2029	1991
KN_3	2140,2084	2130,2037	2037,2031	2010,1974
	2056			
RbN_3	2140,2084	2036,2030	2037,2031	2015,1976
	2056			
CsN_3	2140,2093	2036,2028	2026	2013,2001
	2062			

Table 2 contains IR data from measurements in which different matrix materials were used to prepare disc-shaped samples. It is clear that Li^+ and Na^+ behave irregularly as compared with the other alkali metal azides. LiN_3 and NaN_3 give four bands in a NaCl matrix, which change with time, particularly in the case of LiN_3. It follows that Li^+ may also exchange readily with Na^+. For the heavier alkali metal azides, one dominating absorption band was observed in KBr, RbCl and CsCl wafers, and the wavelengths of the bands characteristic of the azide groups changed only slightly. In contrast with this anomalic feature, in the ν_2 (bending) vibration region [9, 10] no significant differences were observed between the band positions of the azide, as can be seen in Table 3.

Table 3 Alkali azide IR-bands in the bending vibration region (cm^{-1})

	Matrix			
	NaCl	KBr	RbCl	CsCl
LiN_3	642	642	643	643
NaN_3	638	639	639	638
KN_3	639	649	649, 641	637
RbN_3	643, 639	648, 642	643, 639	638
CsN_3	638, 632	649, 642	638	638

Figure 5 shows the derivatographic patterns of the NaN_3/NaY system. TG curves of pure NaY and NaN_3 and their mixture are displayed. It is clear that the dehydration of NaY zeolite is complete at 600 K, before the decomposition of NaN_3 starts. This derivatographic observation is in agreement with our earlier result based on monitoring of the pressure in the reactor system [1]. This behavior was the background of our kinetic measurements since for kinetic study the zeolite should be dehydrated before elementary Na is generated from NaN_3 decomposition. Thus, the generated Na atoms could react exclusively with Brönsted acidic OH groups and not with zeolitic water, since this had been

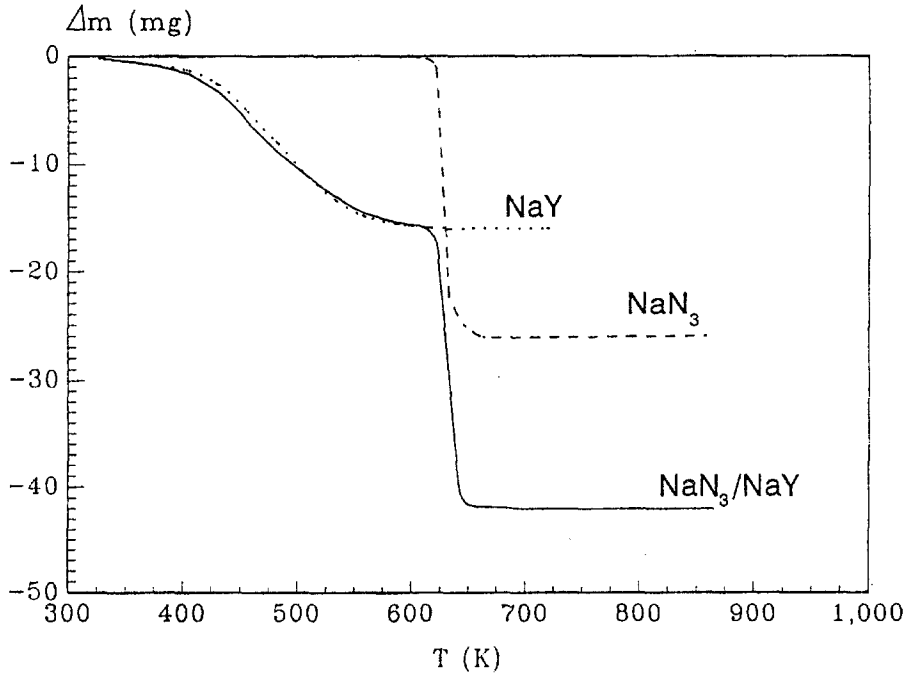

Fig. 5 TG profiles of NaY, NaN_3 and NaN_3/NaY

removed. The pattern shown in this Figure indicated the stoichiometric decomposition of NaN_3.

The derivatographic results in Fig. 6 point to a different character from that obtained for NaN_3-loaded zeolite. Here, for the LiN_3/NaY system, the dehydration temperature of NaY coincides with the decomposition temperature of LiN_3 (508 K), as can be seen from the TG patterns of the pure materials. From this, it might have been concluded that there is no real chance for removal of the water before azide decomposition, but fortunately this is not the case. As the TG curve of the LiN_3/NaY system shows, there is a second mass loss step at around 660 K, which should be due to the decomposition of azide. This is the temperature of azide decomposition in the NaN_3/NaY system as well. Consequently, stabilization of LiN_3 or solid-state ion-exchange should take place, resulting in an increase of the decomposition temperature to that of NaN_3.

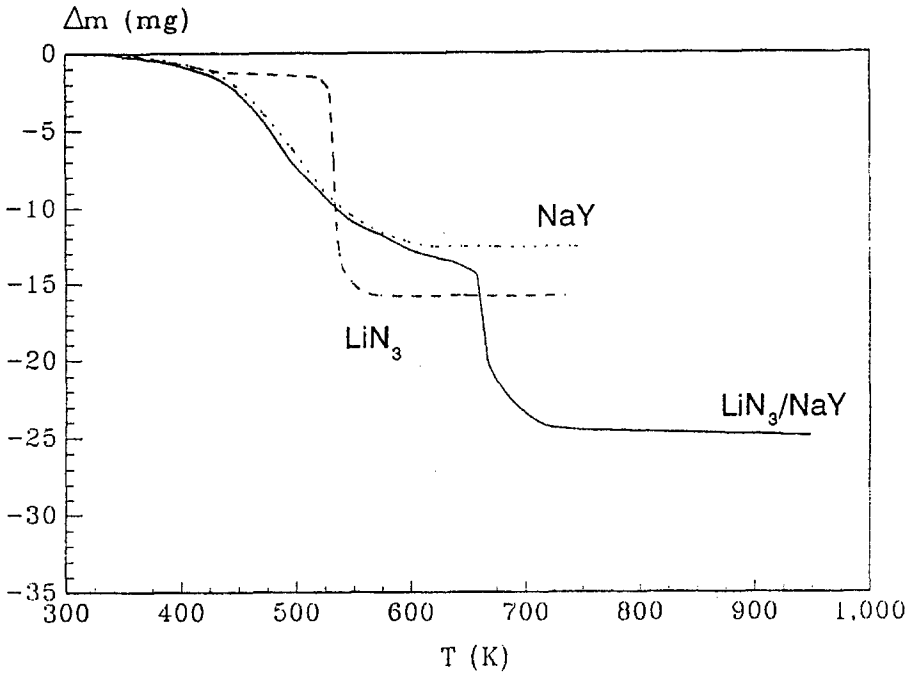

Fig. 6 TG profiles of NaY, LiN_3 and LiN_3/NaY

Figure 7 shows the TG profiles of the CsN_3/NaY system. Here again, the dehydration temperature (508 K) is lower than for the other mass loss steps. It is interesting that in this case no distinct steps can be seen for the CsN_3/NaY system. Simultaneous dehydration and decomposition are presumed to takes place, since the rate of mass loss is smaller than for pure NaY and larger than for pure CsN_3 in the temperature range 298–600 K. A sharp decrease in mass is found at 718 K, above the decomposition temperature of pure CsN_3 (678 K). The final

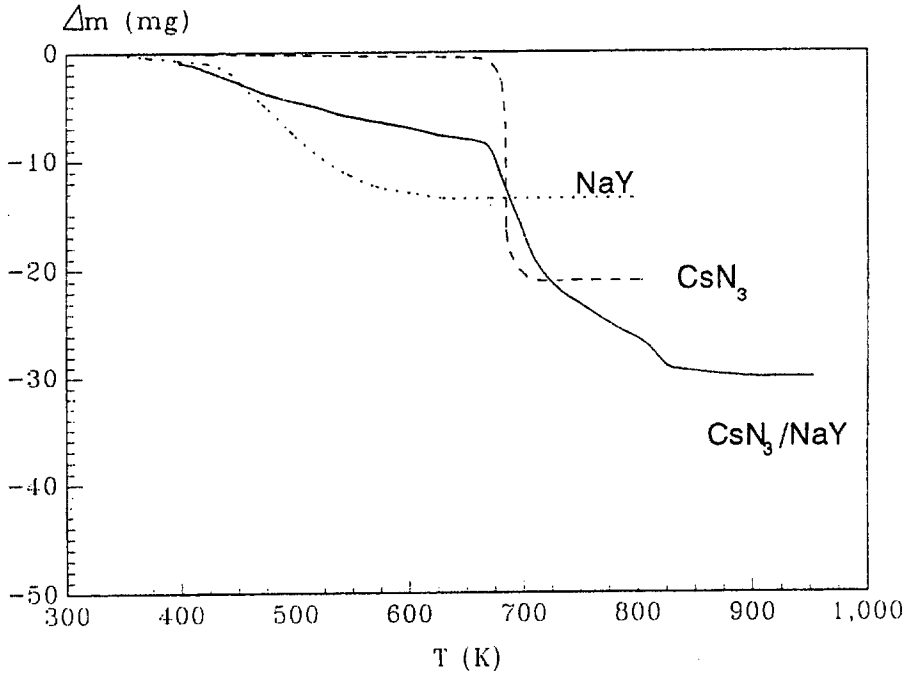

Fig. 7 TG profiles of NaY, CsN_3 and CsN_3/NaY

mass loss step appears at 813 K. We assume that these two mass loss steps, at 718 and 813 K, are due to the decomposition of azide partially or slightly stabilized in the zeolite cages. Here, the stabilization characterized by the higher difference in decomposition temperature is much smaller (40 and 135 K) than for the LiN_3/NaY system (155 K). This deviation may be due to the difference between the ionic diameters of the ions. As Cs^+ is larger than Li^+, its stabilization by occlusion in the small cages of the zeolites may be suppressed to a larger extent.

Earlier, we observed that NaN_3 in zeolite NaY decomposes at a somewhat higher temperature than does pure NaN_3. The difference established was only about 10 degrees, although a very small proportion of the NaN_3 was stabilized in the cages of the zeolite by salt occlusion [2] for materials prepared by impregnation, while no occlusion was observed for mechanically mixed samples. The results presented here and those described earlier are in good agreement as regards the stabilization of azides in the cages of faujasite-type zeolites.

Conclusions

From the results presented in the previous section, the following conclusions can be drawn.

The IR measurements showed that alkali metal azides possess very low thermal stability, hindering even spectroscopic investigations in some instances.

The decompositions of alkali metal azides cannot be described by a uniform feature, though some common characteristics were observed.

The decomposition of azide in a zeolite matrix takes place above the temperatures characteristic for pure LiN_3 and CsN_3. This temperature for NaN_3 exceeds that for pure NaN_3 by only some degrees.

The only common characteristic was the stabilization of the azides in the zeolite cavities, which was earlier observed only for the NaN_3/NaY system.

* * *

The financial support of the National Science Foundation of Hungary (OTKA 1604/91) is gratefully acknowledged.

References

1 P. Fejes, I. Hannus, I. Kiricsi and K. Varga, Acta Phys. Chem. Szeged, 24 (1978) 119.
2 I. Kiricsi, I. Hannus, A. Kiss and P. Fejes, Zeolites, 2 (1982) 247.
3 I. Hannus, Gy. Tasi, I. Kiricsi, J. B. Nagy, H. Förster and P. Fejes, Thermochim. Acta, 249 (1995) 285.
4 M. Brock, C. Edwards, H. Förster and M. Schröder, Stud. Surf. Sci. Catal., 84 (1994) 1515.
5 I. Hannus, I. Kiricsi, A. Béres, J. B. Nagy and H. Förster, Poster abstract, Recent Research Report, 10th Intern. Zeolite Congr., Garmisch Partenkirchen, 1994.
6 L. R. M. Martens, P. J. Grobet and P. A. Jacobs, Nature, 315 (1985) 568.
7 L. R. M. Martens, P. J. Grobet, J. M. Vermeiren and P. A. Jacobs, Stud. Surf. Sci. Catal., 28 (1986) 935; 31 (1987) 531.
8 B. Xu and L. Kevan, J. Chem. Soc. Faraday Trans., 1, 87 (1991) 2843, 3157.
9 J. I. Briant, J. Chem. Phys. 11 (1964) 3195.
10 M. L. Malhotra, K. D. Möller and Z. Iqbal, Physics Letters, 2 (1970) 73.
11 Comprehensive Inorganic Chemistry, Pergamon Press, New York 1973, Vol. 1, p. 438.
12 Gmelins Handbuch der Anorganische Chemie, Verlag Chemie, Weinheim Bergstr. und Berlin, 1937 (1955), Vol. 24. p. 113., Vol 25. p. 115.